q_∞ = adsorbate concentration in equilibrium with c_o, lb.-moles/lb. adsorbent
r = equilibrium parameter of Hiester and Vermeulen, dimensionless
s = column capacity parameter, $\kappa v\epsilon/F$, dimensionless
t = time, sec.
t_H = solution-capacity parameter, $\kappa(V - v\epsilon)/D_G F$, dimensionless
t_H/s = throughput parameter, $(V - v\epsilon)/D_G v\epsilon$, dimensionless
u = parameter defined by Equation (7)
v = bulk-packed volume of column, cu. ft. $v\epsilon$ is the void volume of the column
V = volume of gas fed to column, cu. ft.
W_B = weight of adsorbent bed, lb.
x = bed length parameter, $3D\ D_G v\epsilon/b^2F$, dimensionless
y = contact time parameter, $2D(V - v\epsilon)/b^2F$, dimensionless
z = bed depth, ft.

Greek Letters

ϵ = ratio of void space outside adsorbent particles to total volume of packed bed, dimensionless
κ = general rate coefficient, sec.$^{-1}$
μ = viscosity of gas, lb./(sec.)(ft.)
v/x = external resistance parameter of Rosen, dimensionless
ρ = fluid density, lb./cu. ft.
ρ_B = bulk density of bed, lb. adsorbent/cu. ft.
Φ = shape factor for nonspherical particles, dimensionless

LITERATURE CITED

1. Geser, J. J., and L. N. Canjar, *A.I.Ch.E. J.*, **8**, 494 (1962).
2. Camp, D. T., Ph.D. dissertation, Carnegie Inst. Technol., Pittsburgh, Pa. (1963).
3. Hougen, O. A., and K. M. Watson, "Chemical Process Principles," Pt. III, p. 987, Wiley, New York (1947).
4. Hiester, N. K., and Theodore Vermeulen, *Chem. Eng. Progr.*, **48**, 505 (1952). See also J. H. Perry et al., eds., "Chemical Engineers' Handbook," 4 ed., pp. 16-32, McGraw-Hill, New York (1963).
5. Thomas, H. C., *Ann. N. Y. Acad. Sci.*, **49**, 161-182 (1948).
6. Glueckauf, E., *Trans. Faraday Soc.*, **51**, 1540 (1955).
7. ———, and J. I. Coates, *J. Chem. Soc.*, 1315 (1947).
8. Rosen, J. B., *J. Chem. Phys.*, **20**, 387 (1952).
9. ———, *Ind. Eng. Chem.*, **46**, 1590 (1954).
10. Campbell, M. L., and L. N. Canjar, *A.I.Ch.E. J.*, **8**, 540 (1962).
11. Moison, R. L., and H. A. O'Hern, *Chem. Eng. Progr. Symposium Ser. No. 24*, **55**, 71 (1959).
12. Rimpel, A. E., Ph.D. dissertation, Carnegie Inst. Technol., Pittsburgh, Pa. (1964).

Manuscript received January 27, 1964; revision received October 12, 1965; paper accepted October 20, 1965. Paper presented at A.I.Ch.E. Memphis meeting.

Bubble Shapes in Nucleate Boiling

M. A. JOHNSON, JR., JAVIER DE LA PEÑA, and R. B. MESLER

University of Kansas, Lawrence, Kansas

An attempt is made to explain the differently shaped bubbles observed growing on a surface during nucleate boiling of water. Some of the bubbles photographed were very close to the spherical shape, while others were close to the hemispherical. Also, a number of bubbles had intermediate shapes and were called oblate bubbles.

Measurements of bubble dimensions and growth rates obtained from high-speed films were analyzed. By using a modified Rayleigh equation, the relative importance of the inertial and surface tension forces was computed. It appeared that the differences in shapes among bubbles can be explained on the basis of the relative importance of these forces.

It was found that for spherical bubbles inertial forces are small because of the slow growth rate and surface tension is clearly the dominant force. For hemispherical bubbles, however, the fast growth rate causes a very large inertial force which is greater than surface tension. For the oblate bubbles neither of the forces was found to be dominate and inertia as well as surface tension determines the shape.

In the understanding of nucleate boiling, a better knowledge of bubble behavior is desirable. Many aspects of the study of bubbles, such as growth rate, maximum size, and forces acting on a bubble, have been profusely studied by many different investigators. There has been no attempt, however, to explain the different shapes of bubbles growing on a surface, even though several authors have mentioned and photographed them. The forces acting on a bubble determine the bubble shape. Hence, a study of bubble shapes will probably be of great value in understanding the forces. The purpose of this paper is to call attention to this problem of bubble shapes, which the authors think has not been properly recognized, and to attempt an explanation of bubble shapes in their early stages of growth.

In the early studies of bubbles, spherical shapes were frequently assumed. High-speed photography has shown that this assumption is good in many cases. Shapes very close to the spherical have been reported by Roll (*13*), Keshock and Siegel (*9*) and others. However, Griffith (*3*), Gunther and Kreith (*4*), Han (*5*), Roll (*13*) and Chun (*2*) photographed bubbles that, at least at the early stages of growth, were far from being spherical.

The large number of possible shapes of bubbles growing on a plate may be classified as spherical, hemispherical, or oblate. Sequences of photographs illustrating the three different types of shapes are shown in Figure 1.

It should be mentioned at this point that the shapes predicted by the classical work of Bashforth and Adams (*1*) for static bubbles do not agree with the shapes photographed in this study. Bashforth and Adams obtained bubble shapes that are either nearly spherical or taller and narrower than the bubbles shown in Figure 1. As will be seen later, inertial forces are dominant during the early stages of growth of many bubbles. These forces were not taken into account by Bashforth and Adams and therefore

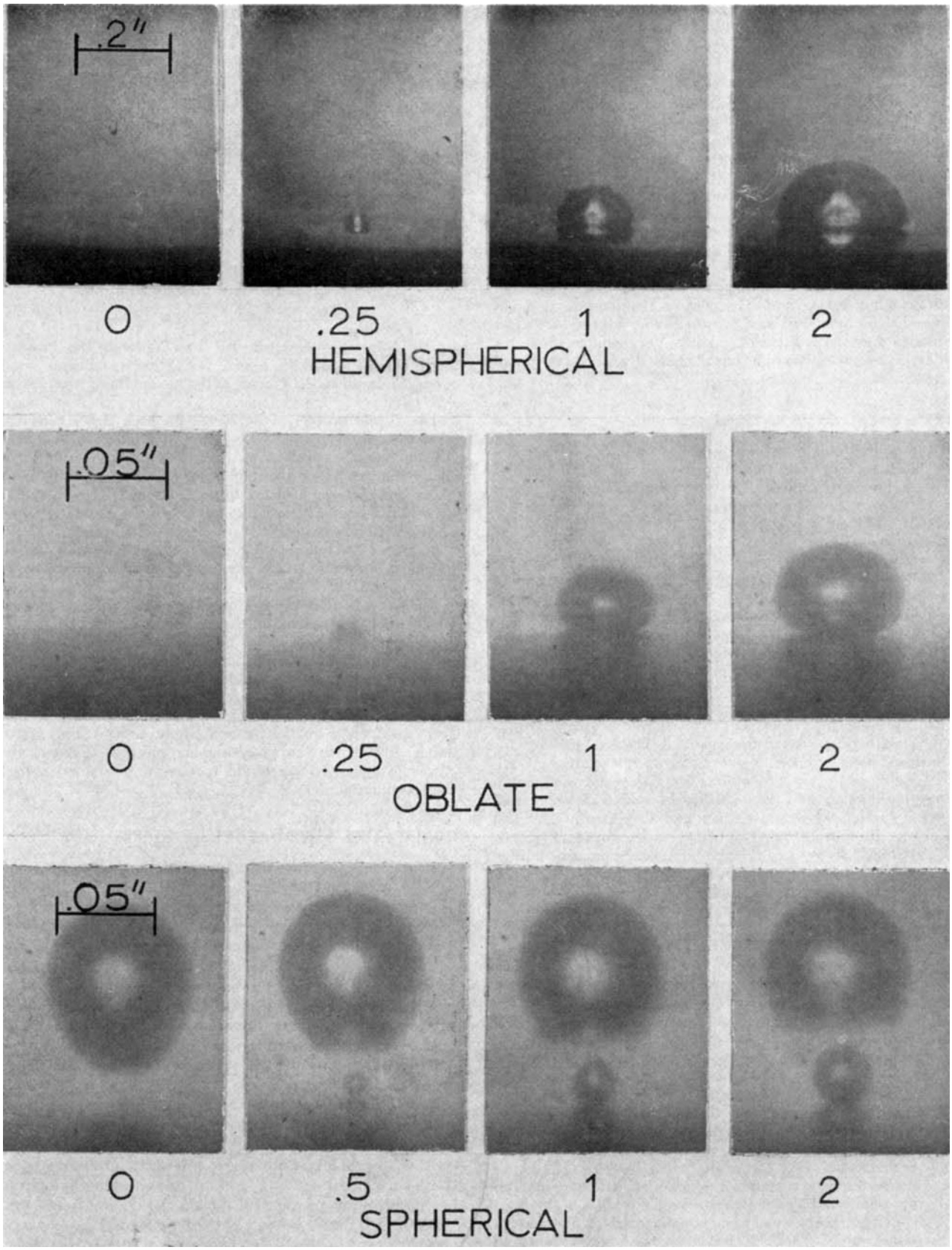

Fig. 1. Sequences of photographs of differently shaped bubbles. (Numbers indicate milliseconds after first picture.)

the application of their results to fast growing bubbles is questionable.

EXPERIMENTAL WORK

In the study of bubbles and of the nucleate boiling mechanism high-speed photography has been a very useful tool. High-speed cameras have made it possible to obtain films from which bubble shapes and their variations with time can be studied.

The experimental work on which this analysis is based was done by one of the authors (M. A. J.) using a Fastax WF-17 combination oscillo-streak and framing camera with a speed of 4,000 frames/sec. Boiling of water was produced by electrically heating a highly polished metal surface of Chromel P on which a hole of 0.0016 in. diameter was drilled to serve as artificial nucleation site. The surface temperature was not measured. The heat flux at the surface was adjusted to allow bubbles to grow from the artificial site. Very similar apparatus and experimental procedure have been described in detail by Rogers and Mesler (*12*).

EXPERIMENTAL OBSERVATIONS

While boiling at atmospheric pressure and with a heat flux of 19,200 B.t.u./(hr.)(sq. ft.), the spherical and oblate bubbles in Figure 1 were obtained. The hemispherical bubbles, shown also in Figure 1, were obtained under a pressure of 0.4 lb./sq. in. abs. and a heat flux of 73,300 B.t.u./(hr.)(sq. ft.) in a later experiment.

Operating pressure and heat flux, both of which can be arbitrarily fixed by the investigator, determine the driving force for the boiling. Because of this, these two factors are of special importance in determining the bubble shape. But also some other factors, which cannot be controlled, appeared to be related to bubble shape. Among these latter factors are growth rate, size of departing bubbles, delay time, and contact diameter. The variations in shape observed while operating under the same pressure and heat flux can only be explained by these latter factors.

The growth rate is small for spherical bubbles but large for the hemispherical bubbles. Figure 2 shows the relative growth rates for differently shaped bubbles. In Figure 2*a* the growth rates of three oblate and three spherical bubbles are compared. These six bubbles were consecutive and alternatively spherical and oblate. In spite of being obtained under the same operating conditions there is a clear difference between bubble growth rates for oblate and for spherical bubbles. Figure 2*b* shows the growth rates for hemispherical and spherical bubbles. Oblate bubbles have intermediate growth rates between these two extreme cases.

For the spherical and the oblate bubbles, two different periods of growth can be observed: a first period of very fast growth followed by a second period of a much slower growth rate. For the spherical and oblate bubbles shown in Figure 2*a*, the steep curves (up to 1 or 2 msec.) correspond to the fast growth of the first period. Sometime between 1 and 2 msec. a change in slope can be observed and after that the second period of slow growth begins. This change in slope is more clearly seen in a plot of log R vs. log t. For the hemispherical bubbles, however, only the first period seems to exist. An explanation of this apparent anomaly is given later.

Another interesting difference between bubbles of different shapes is the relative size of the departing bubbles. The hemispherical are the largest, while the spherical are the smallest. Again, the oblate bubbles have intermediate values.

Delay time is probably the most influential of the factors controlling bubble shape. Delay time, also called waiting period, is the time between the departure of a bubble and the first appearance of a new one at the same nucleation site. It has already been reported by several investigators (*7, 16*), and was also found in this study, that the delay time is not necessarily equal to the bubble growth period as Jakob (*8*) reported.

Spherical bubbles are only observed when there is a very small delay time, that is, very little or no time between consecutive bubbles. For relatively large delay times only oblate or hemispherical bubbles were photographed. For example,

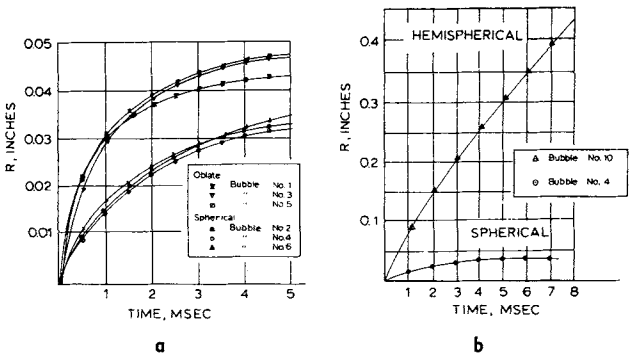

Fig. 2. Comparison of bubble growth rates.

for the oblate bubbles 1, 3, and 5 of Figure 2*a* the delay times were 57, 51, and 45 msec., respectively, whereas for the spherical bubbles 2, 4, and 6 the delay times were at most 0.25 msec.

The slower growth of bubbles with little delay time agrees with the results reported by Hsu and Graham (*7*). Three of the bubbles that they report had delay times of 0 to 0.0018 sec. Photographs of these bubbles are not presented in the paper but their small delay time, their small growth rate, and their small sizes at departure indicate that these bubbles are most probably spherical.

Sequences of bubble photographs showing an oblate bubble followed immediately by a spherical bubble have also been reported by Griffith (*3*).

The contact diameter is a measure of the area of the bubble which is in contact with the hot surface. It can be easily visualized that the spherical bubbles have small contact diameter, whereas for the hemispherical bubbles the contact diameter is close to twice the height of the bubble.

The preceding observations are not only based on the relatively few bubbles for which data are given here. They are also based on a qualitative analysis of several films obtained under different operating conditions and by different investigators. No bubble was found to have a behavior opposed to the one reported here.

QUALITATIVE EXPLANATION OF SHAPES

It appears that the differences in shapes among bubbles can be explained on the basis of the relative importance of inertia and surface tension forces.

Because of the fastest growth, the hemispherical bubbles have the largest inertial forces. The inertial forces dictate a spherically symmetric flow. On the surface, this leads to a hemispherical shape.

For slow growths the inertial forces are smaller and the surface tension, being the dominant force acting on the bubble, imposes the spherical bubble shape.

The oblate bubbles are intermediate between the two preceding cases.

It is a proven fact (*6, 12*) that there is a quick drop in surface temperature every time that a bubble begins its growth and then a slower recovery. Bubbles following quickly one after another are spherical, probably because they start their growth before the surface temperature has had time to recover fully from the cooling effect of the preceding bubble. Since the surface would be cooler, the vapor pressure would be less which then gives a lower growth rate and, thus, a spherical bubble.

As mentioned before, there are two periods in the growth of a bubble: one of fast growth followed by another of much slower growth. For the first period inertial forces can be dominant and, if this is the case, the bubble is hemispherical or at least of the oblate type. But if the growth is not fast enough the surface tension forces are dominant even during this first period and the bubble is spherical throughout all its growth.

As the bubble grows the inertial forces decrease very rapidly. The surface tension force also decreases due to the larger radii but not as quickly as the inertial forces. The result is that sometime during the second period the surface tension takes over and gradually the bubble becomes more spherical. After that the bubble is ready for the detachment stage, which will not be considered here.

QUANTITATIVE EXPLANATION OF SHAPES

A number of bubbles of a film were selected and their principal dimensions, width A, height B, and contact diameter C, shown in Figure 3, were measured for all the pictures of each bubble. Dimensions A, B, and C change with time as shown in Figure 4 for a spherical and for an oblate bubble. Note that for spherical bubbles A and B have very similar growth rates, whereas for oblate bubbles A grows faster initially than B. Note also that A levels off, whereas B keeps growing until bubble departure. The contact diameter C grows during the fast growth period, goes to a maximum, and decreases during the late period to a zero value when the bubble departs.

A difficulty appeared when trying to construct the growth curve of the bubble: that of assigning the zero time, that is, the time when the bubble starts growing. Neither to the first frame in which the bubble appears nor to the frame before it should the zero time be assigned, because the bubble starts its growth some time *within* the lapse of time between the two frames. The error can never be greater than 0.25 msec. (time between frames) but it might be close to it and that would be a relatively important time because of the fast initial growth. This error was considerably diminished by the following procedure. The equivalent radius, which will be defined later, was plotted as a function of arbitrary time based on considering $t = 0$ for the frame immediately before the bubble appears. A smooth curve was then drawn through the points and extrapolated to the time axis. The origin of the time axis was then shifted to the intersection point. Smoothed data were read off the curve drawn through the experimental points.

Rayleigh (*10*) derived an equation to predict the rate of collapse of a spherical cavity. A modification of Rayleigh's equation in which surface tension and viscous forces are taken into account is reported by Westwater (*15*). The latter equation is

$$R\frac{d^2R}{dt^2} + \frac{3}{2}\left(\frac{dR}{dt}\right)^2 + \frac{2\sigma}{\rho_1 R} + \frac{4\mu}{\rho_1 R}\frac{dR}{dt} = \frac{\Delta P}{\rho_1} g_c \quad (1)$$

The first two terms account for the contribution of the inertial forces (per unit area) to the total ΔP. The third term is the surface tension contribution and the fourth term accounts for the viscous forces.

For nucleate boiling of water and for the conditions used here, the viscous forces contribution was found to be small for all bubbles. Thus, Equation (1) without the viscous term was used to analyze the data.

Equation (1) is derived for spherical bubbles. It should be directly applicable to the radii of both the spherical and hemispherical bubbles. However, its application to the oblate bubbles is not so direct. Nevertheless, by defining some equivalent radius to characterize the oblate shapes it should be possible to obtain some indication of the behavior. Accordingly, the volume of the oblate bubbles was calculated with the assumption that they were oblate spheroids. The radius of a sphere of this volume was then taken as an equivalent radius for use in Equation (1).

In order to evaluate the inertial contribution, the first and second derivatives of R are needed. Because of the inherent difficulty of differentiating directly numerical data, curves of different types were sought to represent the growth rate of the bubbles. The derivatives were then obtained from the equations of the different curves used. Polynomial, logarithmic, and exponential functions were tried. Sometimes, no one function could be found to represent satisfactorily the entire range. In these cases, the range was divided into overlapping segments and separate functions were used for them.

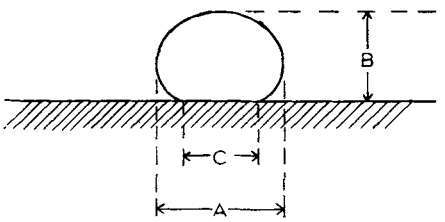

Fig. 3. Bubble dimensions.

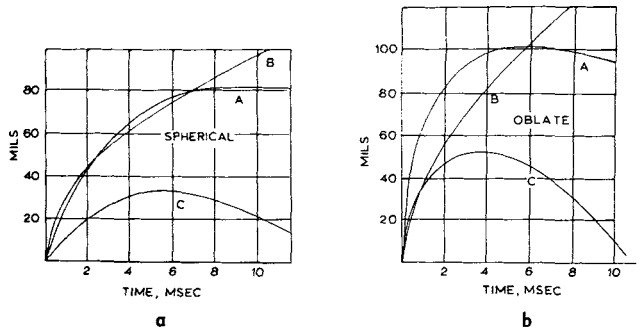

Fig. 4. Time variation of bubble dimensions.

RESULTS AND DISCUSSION

The results, presented graphically in Figure 5, substantiate the qualitative explanation previously given.

Figure 5*a* shows that for spherical bubbles the term accounting for surface tension is always greater than the terms accounting for inertial forces. Notice that although the surface tension term drops very quickly, due to the relatively fast growth of the first period, this term is at any moment greater than the inertial terms. Similar plots were obtained for all the spherical bubbles analyzed.

For hemispherical bubbles Figure 5*b* shows the surface tension term to be very small compared to the inertial terms. At 8 msec. the bubble was still hemispherical but had begun to grow out of the field photographed.

For oblate bubbles Figure 5*c* shows that both forces, surface tension and inertia, have significant influence on the shape. These two forces together dictate the oblate shape. When after 1 or 1.5 msec. the fast growth has ceased, the inertial contribution becomes smaller than the surface tension and the bubble gradually becomes spherical. This is a necessary step before the bubble can pull off the surface.

The microlayer vaporization hypothesis of Moore and Mesler (*11*), to which Sharp (*14*) has added some experimental evidence, is in very good harmony with the experimental observations and with the results reported here. Moore and Mesler postulated the existence of a microlayer of liquid beneath the bubble. The vaporization of this microlayer removes heat from the metal surface very quickly, producing the quick drop in surface temperature recorded by Moore and Mesler (*11*) as well as the initial fast period of growth. When the vaporization of the microlayer is complete further growth would only result from the vaporization at the bubble wall caused by diffusion

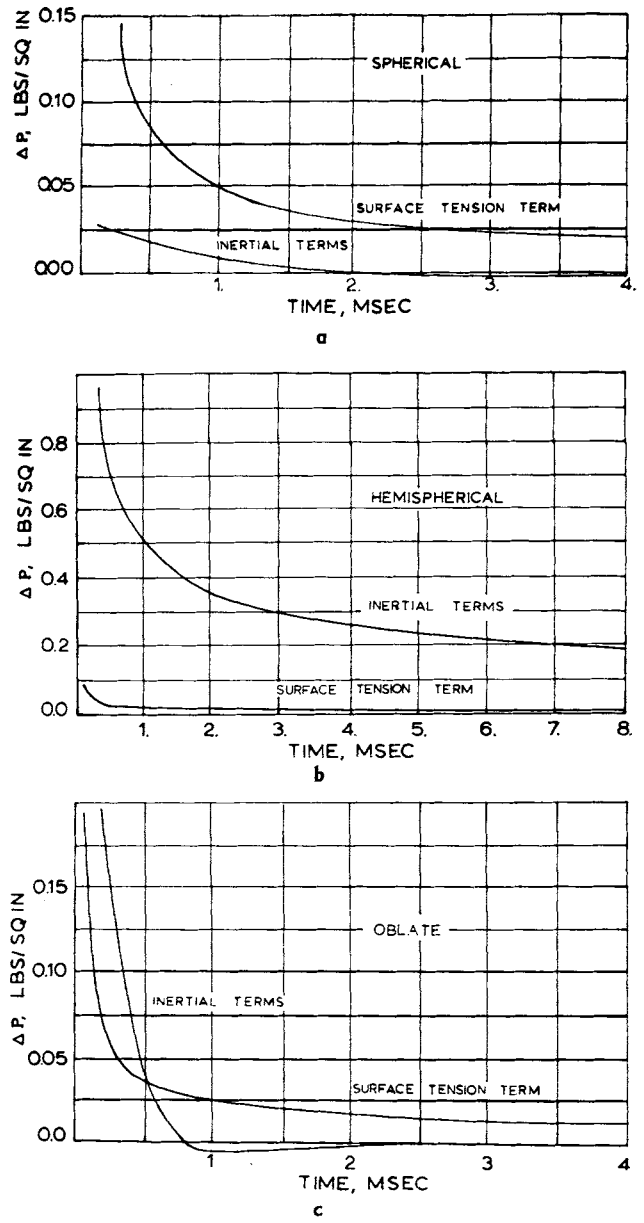

Fig. 5. Contributions to internal pressure.

of heat to the wall from the superheated liquid. This explains why there should be a second period of growth of slower rate.

Hendricks and Sharp (6) report that under low pressures the complete vaporization of the microlayer takes a much longer time. This would explain why, for the hemispherical bubbles reported in this study, only the initial fast period of growth was observed. It would also explain the huge and continuous growth of these bubbles.

In addition, the microlayer hypothesis is consistent with the relation existing between contact diameter, growth rate, and bubble size. Because of the little area of contact, the spherical bubbles benefit less from microlayer vaporization; consequently, their sizes and growth rates are small. For the hemispherical bubbles, on the other hand, the large contact diameter permits more vaporization at the base. This helps to yield the large sizes and fast growth observed for them.

CONCLUSIONS

The following conclusions can be drawn from the preceding analysis of the shapes of bubbles growing on a surface during nucleate boiling of water:

1. Delay time, rate of growth, contact diameter, and size of the bubble at departure are important factors closely related to bubble shape. These factors are not independent. A longer delay time brings about a faster rate of growth, a larger contact diameter, and a bigger size of the bubble at departure.

2. Spherical bubbles have little or no delay time, slow rate of growth, little contact area and small size at departure. Hemispherical bubbles have a long delay time, a very fast rate of growth, a large contact area, and a very large bubble volume at departure. Oblate bubbles have intermediate values for all these factors.

3. It appears that bubble shapes can be explained in terms of inertial and surface tension forces. For spherical bubbles the surface tension force is, at all times, greater than the inertial force, while for hemispherical bubbles the inertial force is the dominant one. For oblate bubbles neither one of them is clearly dominant.

4. Oblate bubbles tend to become spherical before they leave the surface. This happens only when the inertial forces have decreased to a level below the surface tension forces.

NOTATION

g_c = 32.16 $(lb._m)(ft.)/(lb._f)(sec.^2)$
P = pressure in liquid at a distance, lb./sq. in.
P_i = pressure inside bubble, lb./sq. in.
R = radius or equivalent radius of bubble, in.
t = time, sec.
ΔP = pressure difference $P_i - P$, lb./sq. in.
μ = liquid viscosity, lb./(ft.)(sec.)
ρ_l = liquid density, lb./cu. in.
σ = surface tension, lb./in.

ACKNOWLEDGMENT

The National Science Foundation (Grant GP-390), the University of Kansas Computation Center, and the University of Kansas General Research Fund supported this project.

LITERATURE CITED

1. Bashforth, F., and J. Adams, "An Attempt To Test The Theories Of Capillary Action By Comparing The Theoretical And Measure Forms Of Drops Of Fluid," University Press, Cambridge, England (1883).
2. Chun, K. S., Ph.D. thesis, Illinois Inst. Technology, Chicago (1956).
3. Griffith, P., *Massachusetts Inst. Technol. Tech. Rept. No. 8* (June, 1956).
4. Gunther, F. C., and Frank Kreith, *JPL Progr. Rept. No. 4-120* (March 9, 1950).
5. Han, C. Y., and P. Griffith, *Massachusetts Inst. Technol. Tech. Rept. No. 19* (March 30, 1962).
6. Hendricks, R. C., and R. R. Sharp, *Natl. Aeronaut. Space Admin. Tech. Note D-2290* (April, 1964).
7. Hsu, Yih-Yun, and R. W. Graham, *ibid., D-594* (May, 1961).
8. Jakob, Max, "Heat Transfer," pp. 631-632, Wiley, New York (1949).
9. Keshock, E. G., and R. Siegel, *Natl. Aeronaut. Space Admin. Tech. Note D-2299* (August, 1964).
10. Lord Rayleigh, *Phil. Mag.*, **34**, 94 (1917).
11. Moore, F. D., and R. B. Mesler, *A.I.Ch.E. J.*, **7**, 620 (1961).
12. Rogers, T. F., and R. B. Mesler, *ibid.*, **10**, 656 (1964).
13. Roll, J., Ph.D. thesis, Purdue Univ., Lafayette, Ind. (1963).
14. Sharp, R. R., *Natl. Aeronaut. Space Admin. Tech. Note D-1997* (1964).
15. Westwater, J. W., *Am. Scientist*, **47**, 427 (1959).
16. ———, and D. B. Kirby, *Chem. Eng. Progr. Symposium Ser. No. 57*, **61**, 238-248 (1965).

Manuscript received March 8, 1965; revision received November 15, 1965; paper accepted November 16, 1965. Paper presented at A.I.Ch.E. Los Angeles meeting.